



## Dynamic studies of CO oxidation on nanoporous Au using a TAP reactor

L.C. Wang<sup>a</sup>, H.J. Jin<sup>b,1</sup>, D. Widmann<sup>a</sup>, J. Weissmüller<sup>b,2</sup>, R.J. Behm<sup>a,\*</sup>

<sup>a</sup>Institute of Surface Chemistry and Catalysis, Ulm University, D-89069 Ulm, Germany

<sup>b</sup>Karlsruher Institute of Technology, Institute of Nanotechnology, D-76344 Eggenstein-Leopoldshafen, Germany

### ARTICLE INFO

#### Article history:

Received 3 August 2010

Revised 5 December 2010

Accepted 8 December 2010

Available online 22 January 2011

#### Keywords:

Nanoporous Au catalysts

CO oxidation

Oxygen storage capacity (OSC)

Dynamic studies

Temporal analysis of products (TAP)

### ABSTRACT

The oxidation of CO on nanoporous Au (NPG), in particular the activation of molecular O<sub>2</sub>, was investigated by a combination of kinetic and temporal analysis of products (TAP) measurements. Continuous reaction measurements in a flow of reaction gas, at atmospheric pressure, show a catalytic behavior of the NPG, with the activity decreasing to 33% of the initial activity over 1000 min on stream. In contrast, during simultaneous pulsing of CO and O<sub>2</sub>, the formation of CO<sub>2</sub> on the NPG catalyst rapidly decreased to values below the detection limit after reactive removal of the surface oxygen species present after sample preparation. Possible mechanisms explaining this discrepancy are discussed, using further information from multi-pulse TAP experiments, which revealed that molecular O<sub>2</sub> can be activated and stored on NPG catalyst at room temperature, though with a low probability.

© 2010 Elsevier Inc. All rights reserved.

### 1. Introduction

Oxide-supported Au catalysts with Au nanoparticles of a few nanometers in diameter have been the subject of numerous studies since the early reports by Haruta et al. about their high activity in various oxidation and reduction reactions already at low temperatures [1,2], most prominently the CO oxidation reaction [3–5]. Despite extensive research efforts, the debate about the physical origin of their high activity as well as the underlying mechanisms still continues. While there seems to be a general consensus that apart from the Au particle size [6,7], the interaction between Au nanoparticles and oxide support plays an important role for the high activity of these Au catalysts ('interface pathway' [8,9]), other mechanisms such as reaction at undercoordinated Au sites ('Au only pathway' [9]) have been proposed and substantiated as well [10,11]. In the end, more than one reaction pathway may contribute to the reaction [12]. For the interface pathway, it is often assumed that the active sites are the perimeter sites at the interface between Au particles and oxide support and that (molecular) oxygen can be activated at these sites [9,13]. In recent quantitative measurements in a temporal analysis of products (TAP) reactor, we could indeed demonstrate that on various oxide-supported Au catalysts, active oxygen species can be reversibly stored

and reactively removed upon alternative exposure to O<sub>2</sub> and CO pulses [13–16]. Furthermore, for Au/TiO<sub>2</sub>, both the oxygen storage capacity (OSC) and the reactivity of the Au/TiO<sub>2</sub> catalysts showed an almost linear relationship with the perimeter of the interface between Au nanoparticles and TiO<sub>2</sub> support, providing first direct support for the above mechanistic proposal (reaction at perimeter sites) [13].

Recently, it has been reported that monolithic nanoporous gold (NPG) prepared by leaching of Ag from an AuAg alloy also exhibits a remarkably high activity for CO oxidation [17–20]. In the absence of any support materials, it seems that interactions between metal oxide support and gold and the resulting interface sites are not mandatory for the catalytic activity of Au catalysts. On the other hand, based on the results of detailed reaction kinetic studies, Wittstock et al. suggested that the residual Ag on the surface of NPG catalysts plays a significant role in activating molecular oxygen and that these NPG catalysts should be considered as a bimetallic catalyst rather than a pure Au catalyst [18,21]. However, details of the reaction mechanism are unclear, in particular the nature of the active oxygen species and the active sites for O<sub>2</sub> activation.

In this paper, we report results of a combined micro-reactor and TAP reactor study on the kinetics and transient reaction behavior of the oxidation of CO over nanoporous Au catalysts. Following the description of the kinetic measurements in a micro-reactor, we present results of dynamic measurements in a TAP reactor in order to clarify whether these catalysts are also able to activate molecular oxygen and, if so, whether the amount of stored reactive oxygen (oxygen storage capacity – OSC) is correlated with the catalytic activity for CO oxidation of the respective catalysts, as it has been demonstrated for oxide-supported Au catalysts [13–16].

\* Corresponding author. Fax: +49 731 50 25452.

E-mail address: [juergen.behm@uni-ulm.de](mailto:juergen.behm@uni-ulm.de) (R.J. Behm).

<sup>1</sup> Present address: Institute of Metal Research, Chinese Academy of Sciences, Shenyang, PR China.

<sup>2</sup> Present address: Institute of Materials Physics and Technology, Hamburg Technical University, D-21073 Hamburg, Germany.

## 2. Experimental

### 2.1. Nanoporous gold sample preparation

Nanoporous gold samples were prepared by electrochemical etching (dealloying) of an Ag–Au alloy, as reported previously [22,23]. The master alloy Ag<sub>75</sub>Au<sub>25</sub> (at.%) was prepared by arc melting of high-purity Au and Ag wires (Au 99.9985% and Ag 99.99%, Chempur) and subsequent homogenization at 950 °C for 50 h (sealed in a quartz tube). Rectangular samples of about  $1.8 \times 1 \times 1 \text{ mm}^3$  in size were cut from the ingot and annealed at 850 °C for 1.5 h under Ar for recovery. Dealloying was performed in 1 M HClO<sub>4</sub> aqueous solution, at a potential of 0.85 V (with respect to an Ag/AgCl reference electrode placed directly in the 1 M HClO<sub>4</sub> electrolyte close to the sample) for approximately one day. To minimize silver contamination in the sample compartment, the coiled-Ag wire counter electrode (CE) was separated from the main cell by placing it in a tube filled with the same solution and mounted with its opening close to the sample. The dealloying was stopped when the current fell to 10  $\mu\text{A}$ . After dealloying, the electrolyte was replaced by new base electrolyte and a higher potential (0.95 V) was applied to the sample for a few hours to further remove the silver (ions) which had remained in the pore channels. Subsequently, the cell was repeatedly rinsed with fresh 1 M HClO<sub>4</sub> to remove traces of Ag ions in solution. The NPG disks were crushed and gently ground into powder before use.

### 2.2. Catalyst characterization

Since the microstructure of the NPG samples may be destroyed under the normal conditions of a BET measurement, the surface area of as-prepared NPG material was determined via the capacitance ratio method [24], yielding a value of  $75 \pm 5 \text{ m}^2 \text{ g}^{-1}$ . The surface morphology, microstructure and the bulk concentration of Ag were determined by scanning electron microscopy (SEM) and energy dispersive X-ray spectroscopy (EDX), respectively. X-ray photoelectron spectroscopy (XPS) data were recorded on a PHI 5800 ESCA system (Physical Electronics) using monochromatic Al K $\alpha$  radiation.

### 2.3. Catalytic activities measured on the flow reactor

The catalytic activity of the NPG catalyst for CO oxidation was measured in a micro-reactor with a length of 300 mm, an outer diameter of 6 mm and an inner diameter of 4 mm at atmospheric pressure at 30 °C, without applying any pretreatment prior to the measurements. One milligram of the catalyst was diluted with  $\alpha\text{-Al}_2\text{O}_3$  (1:60) in order to obtain differential reaction conditions, resulting in conversions of below 15% of the reactants during the catalytic measurements. For comparison, the activity of a 3 wt.% Au/TiO<sub>2</sub> catalyst was also measured under the same reaction conditions. The catalyst was diluted with  $\alpha\text{-Al}_2\text{O}_3$  (1:50) and pretreated by calcination in 10% O<sub>2</sub>/N<sub>2</sub> at 400 °C for 30 min before reaction. The temperature of the catalyst bed is measured by a thermo couple attached to the outer wall of the reactor, centered along the catalyst bed. The flow rate of reactant gas was 60 Nml min<sup>-1</sup> (1% CO, 1% O<sub>2</sub>, rest N<sub>2</sub>), and both influent and effluent gases were analyzed by on-line gas chromatography (DANI, GC 86.10). For further details on the setup and the evaluation, see Ref. [25].

### 2.4. TAP measurements

The pulse experiments were carried out in a home-built TAP reactor [26], which is largely based on the TAP-2 approach of

Gleaves et al. [27]. In short, piezo-electric pulse valves were used to generate gas pulses of typically  $\sim 1 \times 10^{16}$  molecules per pulse. For all measurements presented, these pulses contained 50% Ar as an internal standard to enable quantitative evaluation on an absolute scale. The gas pulses were directed into a quartz tube micro-reactor with a length of 90 mm, an outer diameter of 6 mm and an inner diameter of 4 mm. The catalyst bed was located in its central part and was fixed by two stainless steel sieves (Haver & Boecker OHG, transmission 25%). For all measurements, we used a three-zone catalyst bed containing 2 mg of NPG catalyst diluted with 20 mg SiO<sub>2</sub> as central zone and two layers of SiO<sub>2</sub>, as outer zones (total mass 150 mg). All pulse experiments were performed at 30 °C reaction temperature. Here too, the catalyst was used as received, with no additional pretreatment prior to the measurements. After passing through the reactor, the gas pulses are analyzed by a quadrupole mass spectrometer (QMG 700, Pfeiffer) located behind the reactor tube in the analysis chamber. The consumption of CO and O<sub>2</sub> in the respective pulses was calculated from the missing mass spectrometric intensity in the pulses compared to the intensity after saturation, which is equivalent to the initial intensity. The formation of CO<sub>2</sub> could be determined directly from the CO<sub>2</sub> pulse intensity. The reactor can be separated from the ultrahigh vacuum (UHV) system by a differentially pumped gate valve and connected directly to an adjustable roughing pump.

In the multi-pulse experiments, the catalyst samples were exposed alternately to sequences of 200 CO/Ar and 200 O<sub>2</sub>/Ar pulses in order to reactively remove and re-deposit active oxygen. Due to experimental reasons, the first pulse in a sequence is typically lower in intensity. For testing the catalytic activity in the TAP reactor, the samples were exposed to simultaneous pulses of CO/Ar and O<sub>2</sub>/Ar. For both measurements, the resulting CO:O<sub>2</sub> ratio was 1:1 and hence there was an excess of oxygen relative to stoichiometric reaction conditions. The measurements with simultaneous pulses were used for comparison with the catalytic activity measured in the micro-reactor. In the experiments using isotope-labeled reactants, a gas mixture of <sup>18</sup>O<sub>2</sub>/Ar was used. Prior to these measurements, it was checked that the gas-mixing unit and the gas pipes containing the reaction mixture as well as the reactor and the dilution materials were inert, and no conversion of CO or O<sub>2</sub> was found under these conditions in control experiments.

To identify carbon-containing adsorbed species accumulated on the catalyst surface during reaction and oxygen species present on the surface before and after the reaction, we also performed temperature-programmed desorption (TPD) measurements in the TAP reactor. The measurements started directly after reaction, heating the catalyst from 30 °C to 600 °C with a heating rate of 25 °C min<sup>-1</sup>. The gaseous desorption/decomposition products are transported by diffusion into the analysis chamber, where the effluent gases are detected by the mass spectrometer.

## 3. Results and discussion

As reported in references [22,28], TEM images demonstrated that the NPG material exhibits a three-dimensional nanoporous microstructure with a uniform ligament size of ca. 4 nm. The ligament size is stable in the initial oxidized state but is expected to grow after reduction. XPS characterization of the as-prepared NPG sample (see Fig. 1a) showed that the binding energy (BE) of the Au(4f<sub>7/2</sub>) state is 84.4 eV, which is slightly higher than the standard BE of metallic Au (84.0 eV) [29,30]. Curve fitting of the Au(4f) signal results in a contribution of ca. 17% from an additional peak at 85.2 eV. The peak at higher BE is assigned to partially oxidized Au species [30]. The Ag(3d) XP spectrum consists of two distinct peaks at 368.4 and 374.4 eV, which are characteristic for metallic Ag<sup>0</sup> [31,32], and additional smaller peaks centered at 367.8 and

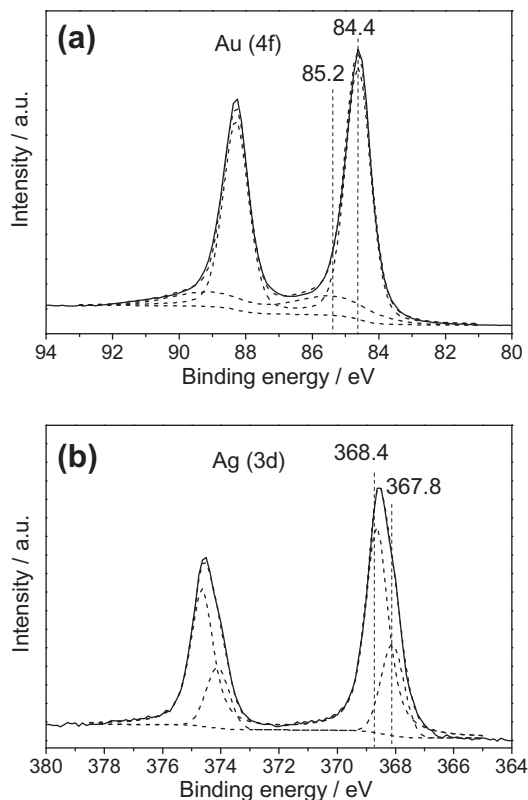


Fig. 1. Au(4f) (a) and Ag(3d) (b) XP spectra of the as-prepared NPG catalyst.

373.8 eV (see Fig. 1b). The latter doublet can be assigned to Ag<sub>2</sub>O [31]; it contributes about 25% to the total Ag(3d) intensity. A quantitative analysis of the XP spectra revealed an Ag surface concentration of 18.6 at.%. This value is slightly higher than the bulk concentration of 14.6 at.% determined by EDX, pointing to a slight enrichment of Ag on the surface after preparation of the NPG catalyst. Similarly, Wittstock et al. [18] also reported an enrichment of Ag at the surface of a NPG catalyst (7 at.%, bulk phase below 1 at.%).

The catalytic activity of the NPG catalyst for CO oxidation was first tested in a conventional micro-reactor at atmospheric pressure. Fig. 2a shows that the initial activity at 30 °C starts out at  $1.8 \times 10^{-4} \text{ mol}_{\text{CO}} \text{ s}^{-1} \text{ g}_{\text{Au}}^{-1}$ . After an initial, fast decay, the activity stabilizes and remains at  $6.2 \times 10^{-5} \text{ mol}_{\text{CO}} \text{ s}^{-1} \text{ g}_{\text{Au}}^{-1}$  after 1000 min on stream. The total deactivation during the reaction time corresponds to ca. 67%. Possible reasons for the deactivation will be discussed later, together with the data from Fig. 9. It should be noted, however, that due to the strong dilution of the catalysts thermal effects caused by the significant exothermicity of the CO oxidation reaction are unlikely. The Au-mass-normalized (final) activity is substantially lower than that of a 3 wt.% Au/TiO<sub>2</sub> catalyst ( $3.4 \times 10^{-4} \text{ mol}_{\text{CO}} \text{ s}^{-1} \text{ g}_{\text{Au}}^{-1}$ , Fig. 2a), reaching about 20% of that under similar reaction conditions (steady-state conditions). Assuming that all surface Au atoms contribute to the activity, the steady-state activity corresponds to a turnover frequency (TOF) of  $0.04 \text{ s}^{-1}$  (Au(1 1 1):  $1.4 \times 10^{15} \text{ atoms cm}^{-2}$ ). Recently, Wittstock et al. [18] conducted catalytic measurements on a NPG disk catalyst with a ligament size of 30–50 nm, yielding a reaction rate of  $1.9 \times 10^{-5} \text{ mol}_{\text{CO}} \text{ s}^{-1} \text{ g}_{\text{cat}}^{-1}$  at 30 °C in a gas mixture of 4% CO, 20% O<sub>2</sub> in He. Since the bulk Ag content is below 1 at.%, this value is identical to the Au-mass-normalized reaction rate. By taking the effect of mass transport into account, these authors estimated a TOF of  $3 \text{ s}^{-1}$  at 20 °C under a gas mixture of 10% CO, >66% O<sub>2</sub> in He. Considering the apparent reaction order of 0.5 for O<sub>2</sub> and values between 0.5 and 1 for the reaction order for CO, with a

tendency to higher values for the samples with higher silver concentrations [18], the much smaller TOF in our case may be caused by the significantly lower concentration of CO (1%) and O<sub>2</sub> (1%) in the feed gas. Xu et al. reported a reaction rate of  $1.3 \times 10^{-5} \text{ mol}_{\text{CO}} \text{ s}^{-1} \text{ g}_{\text{cat}}^{-1}$  for CO oxidation on a powder NPG catalyst at -30 °C reaction temperature, which they calculated from a CO conversion of up to 70% (20 mg catalyst, Ag bulk content ~3 at.%, 1% CO/10% O<sub>2</sub>/89% N<sub>2</sub>, flow rate  $66.7 \text{ ml min}^{-1}$ ) [19,20]. For low values of the activation energy, as they are typical for CO oxidation on Au catalysts, this agrees rather well with our data. Considering the differences in structural characteristics (residual Ag content, surface area) and chemical composition (concentration of reactants, reaction temperature), the variation in activity between different studies are not surprising.

For comparison, the activity of NPG catalyst was also determined by simultaneous pulses of CO/Ar and O<sub>2</sub>/Ar in the TAP reactor under UHV conditions, starting with a fresh catalyst. As illustrated in Fig. 2b, the CO consumption and the formation of CO<sub>2</sub> on the NPG catalyst decreased continuously and eventually were below detection levels (<1% of the initial activity) after 1000 pulses. At the same time, we could not detect any significant O<sub>2</sub> uptake during the pulse reaction. Hence, in this experiment, CO oxidation proceeds via a non-catalytic process, by reaction of CO with oxygen already present on the NPG catalyst at the beginning of the reaction, which is limited by the diffusion of CO gas into the pore structures. This is completely different from the reaction behavior observed in the micro-reactor measurement. Additionally, the reaction behavior of the NPG catalyst also differs distinctly

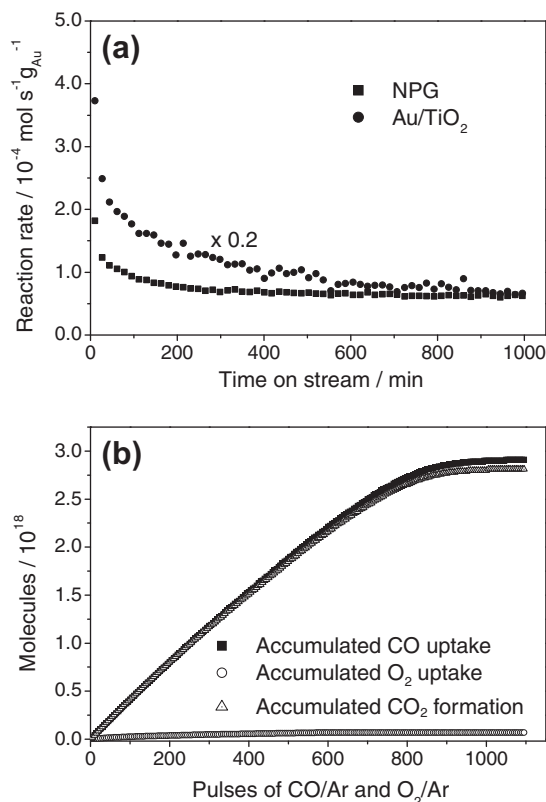


Fig. 2. (a) Catalytic activities of the fresh NPG catalyst and of a 3 wt.% Au/TiO<sub>2</sub> catalyst measured in a micro-reactor under differential reaction conditions as a function of reaction time (reaction temperature 30 °C,  $60 \text{ Nml min}^{-1}$  1% CO/1% O<sub>2</sub>/98% N<sub>2</sub>, atmospheric pressure). (b) Accumulated uptake of CO and O<sub>2</sub> and CO<sub>2</sub> formation during simultaneous pulsing of CO/Ar and O<sub>2</sub>/Ar pulses on the fresh NPG catalyst in the TAP reactor (2 mg NPG catalyst diluted with SiO<sub>2</sub> (1:10), reaction temperature 30 °C,  $1 \times 10^{16}$  molecules per pulse, with CO:Ar and O<sub>2</sub>:Ar = 1:1).

from that of Au/TiO<sub>2</sub> catalysts, where similar TAP reactor measurements showed a steady catalytic activity [13,15,16].

Following the activity measurement, we conducted a TPD experiment to determine the nature and amount of surface species accumulated during the pulse reaction. For comparison, TPD spectra were also recorded on the fresh NPG catalyst. Fig. 3 shows the desorption curves of H<sub>2</sub>O ( $m/z = 18$ ), CO<sub>2</sub> ( $m/z = 44$ ) and O<sub>2</sub> ( $m/z = 32$ ) before and after reaction. The fresh NPG catalyst exhibits a pronounced O<sub>2</sub> desorption peak with a maximum at 274 °C and a shoulder at around 248 °C. Studies using planar single crystal surfaces under ultrahigh vacuum conditions had shown that desorption of atomic oxygen species from Ag exposed to O<sub>2</sub> at temperatures below 220 °C takes place only at higher temperatures, at 322 ± 25 °C [33–35], whereas atomic oxygen deposited on a Au surface by exposure to ozone or O<sup>+</sup> sputtering normally desorbs at temperatures between 270 and 300 °C [10,36–38]. Therefore, the oxygen desorption peak at 274 °C is assigned to desorption of atomic oxygen species chemisorbed on the Au surface. The O<sub>2</sub> desorption peak almost completely disappeared after the pulse reaction, indicating that the surface atomic oxygen species was depleted by reaction with CO molecules, as had been concluded already from the absence of O<sub>2</sub> consumption during the pulse reaction. H<sub>2</sub>O and CO<sub>2</sub> desorption from the fresh NPG sample started directly after heating, resulting in a broad peak with several maxima (150–280 °C), a sudden drop of the desorption rate at the high temperature of the O<sub>2</sub> desorption peak (295 °C) and a weak broad desorption range between 300 and 500 °C. Also, the amount of desorbed H<sub>2</sub>O and CO<sub>2</sub> decreased significantly after the pulse measurements, pointing to a removal of adsorbed H<sub>2</sub>O and CO<sub>2</sub> or carbonate species during the CO oxidation reaction. In addition to desorption (H<sub>2</sub>O), this may be related to O<sub>2</sub>-stimulated decomposition of surface carbonates [14,39] (adsorbed CO<sub>2</sub> is unstable under UHV conditions and would have desorbed instantaneously). Based on the TPD results, the total number of Au surface atoms

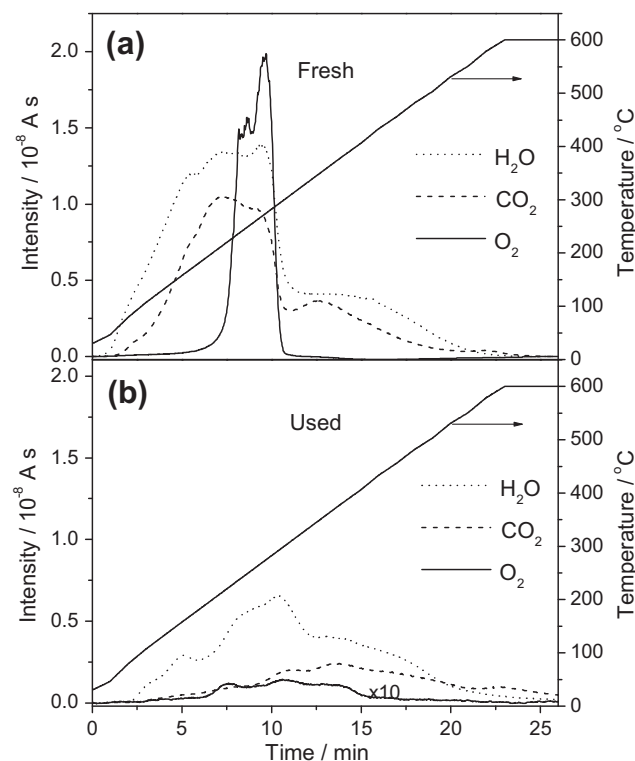


Fig. 3. TPD spectra of the NPG catalyst before and after the simultaneous pulsing experiment shown in Fig. 2b.

(specific surface area 75 m<sup>2</sup> g<sup>-1</sup>, 1.4 × 10<sup>15</sup> atoms cm<sup>-2</sup> on Au(1 1 1)) and assuming that every surface oxygen atom reacts with one CO molecule, nominal oxygen coverages of 1.5 and 0.04 monolayers (ML) can be estimated for the fresh and the used NPG catalyst, respectively.

In order to study the capability of the NPG catalyst to activate O<sub>2</sub> and store active oxygen, we performed multi-pulse experiments by exposing the catalyst alternately to 200 O<sub>2</sub>/Ar and 200 CO/Ar pulses after the removal of the initial surface oxygen. In principle, the OSC of NPG catalyst should be determined directly from the oxygen uptake during O<sub>2</sub> pulsing. However, this method showed a poor reproducibility due to the very low O<sub>2</sub> consumption during these experiments. Therefore, we determined the OSC data from the amount of CO<sub>2</sub> produced upon subsequent CO pulsing (see Fig. 4). The formation of CO<sub>2</sub> (accumulated amount of CO<sub>2</sub> produced or CO consumed, respectively) during pulse titration of a fresh NPG catalyst, after CO pulse reduction and subsequent exposure to 200 pulses of O<sub>2</sub>, is illustrated in curve 1 in Fig. 4 (total amount of stored oxygen: 0.82 × 10<sup>18</sup> O atoms g<sub>Au</sub><sup>-1</sup>). These oxidation–reduction cycles were repeated for 40 times. The CO<sub>2</sub> formation during the following three sequences of O<sub>2</sub> pulsing (200 pulses) and CO pulse reduction are equally shown as curves OSC-2 to OSC-4. During these cycles, the total amount of stored active oxygen decreased considerably, from 0.82 × 10<sup>18</sup> O atoms g<sub>Au</sub><sup>-1</sup> (OSC-1) via 0.60 × 10<sup>18</sup> O atoms g<sub>Au</sub><sup>-1</sup> (OSC-2), 0.53 × 10<sup>18</sup> O atoms g<sub>Au</sub><sup>-1</sup> (OSC-3) to finally 0.51 × 10<sup>18</sup> O atoms g<sub>Au</sub><sup>-1</sup> (OSC-4). This decay continued, until after about 15 pulse sequences the CO<sub>2</sub> formation has essentially reached steady-state conditions, with a reversible OSC of 0.20 × 10<sup>18</sup> O atoms g<sub>Au</sub><sup>-1</sup> (see also Fig. 8). It is well known that the pre-existent atomic oxygen species plays an important role in stabilizing the structure of the NPG catalyst: the surface area of NPG sample was found to decrease by a factor of ca. 15 after removal of the pre-existent oxygen [23]. Therefore, this decrease in the OSC is likely to be associated with a loss of surface area due to a coarsening of the ligaments. This value is about two orders of magnitude lower than the reversible OSC obtained on a 3.4 wt.% Au/TiO<sub>2</sub> catalyst (1.29 × 10<sup>20</sup> O atoms g<sub>Au</sub><sup>-1</sup>, after conditioning in air for 2 h at 400 °C; measurement at 80 °C) [13]. The low activity for oxygen activation fits well to the low CO oxidation activity observed in the simultaneous pulse measurements.

Recently, it was reported that the dissociation probability of O<sub>2</sub> on the herringbone-reconstructed Au(111) surface can be



Fig. 4. Accumulated amount of CO<sub>2</sub> produced on the NPG catalyst during CO pulsing after reduction of a fresh NPG sample (CO pulsing) and 200 pulses of O<sub>2</sub>/Ar within the first 4 and after 15 pulse sequences (200 pulses O<sub>2</sub>/Ar, OSC-1,2,3,4,15) (pulse separation = 4 s).

dramatically increased by the presence of some atomic oxygen on the surface [10]. The dissociation probability of  $O_2$  on Au(1 1 1) containing 0.02 ML  $O_{ad}$  at 127 °C was found to be on the order of  $10^{-3}$ , whereas there was no measurable dissociation on the clean Au(1 1 1) surface [10]. From the OSC data ( $0.2 \times 10^{18}$  O atoms  $g_{Au}^{-1}$  after >15 cycles over 2 mg NPG catalyst) by 200  $O_2/Ar$  pulses with the typical pulse size of the TAP reactor ( $0.5 \times 10^{16}$  molecules  $O_2$  per pulse), the total amount of  $O_2$  molecules activated and exposed can be calculated to be  $0.2 \times 10^{15}$  and  $1 \times 10^{18}$ , respectively. Hence, the average probability for dissociative oxygen adsorption of  $O_2$  can be estimated by dividing the amount of activated  $O_2$  by the  $O_2$  exposure, giving a value of  $0.2 \times 10^{-3}$  for adsorption at 30 °C. On a first view, this may look like a very good agreement with the data by Deng et al. One has to consider, however, that the latter were real sticking coefficients in an UHV experiment with known numbers for surface collisions by exposure to  $^{18}O_2$  for 1 min before measuring the amount of activated  $^{18}O_2$ , giving the probability to adsorb in a single collision with the surface. In contrast, in our case, it refers to an effective sticking probability for an  $O_2$  molecule passing through the catalyst bed rapidly with a contact time of less than 4 s.

Most simply, the very poor catalytic CO oxidation activity of the NPG catalyst in the pulse measurements can be explained by the much lower amount of  $O_2$  available during the reaction compared with continuous reaction at atmospheric pressure. To test for this idea, we exposed the reduced NPG catalyst to different numbers of  $O_2$  pulses and then determined the amount of active adsorbed oxygen formed on the NPG surface by measuring the amount of

$CO_2$  produced upon titration with 50 pulses of  $CO/Ar$ . Experiments on the NPG sample, which were performed after the pulse experiments described above (see Fig. 4), showed that the oxygen uptake increased with the number of  $O_2$  pulses, from  $\sim 0.20 \times 10^{18}$  O atoms  $g_{Au}^{-1}$  after 200 pulses to  $0.59 \times 10^{18}$  O atoms  $g_{Au}^{-1}$  after 1000 pulses,  $1.1 \times 10^{18}$  O atoms  $g_{Au}^{-1}$  after 2000 pulses and  $3.3 \times 10^{18}$  O atoms  $g_{Au}^{-1}$  after 10,000 pulses (see Fig. 5a).

In a second series of experiments, performed on the same NPG sample, we compared the effects of  $O_2$  pulsing with that of continuous exposure to  $O_2$  at atmospheric pressure in a flow of 10%  $O_2/N_2$  (20 ml  $min^{-1}$ , 30 °C, Fig. 5b). The accumulated  $CO_2$  formation after pre-exposure to 2000  $O_2$  pulses is shown in curve a. ( $1.1 \times 10^{18}$  O atoms  $g_{Au}^{-1}$ ). Continuous exposure to  $O_2$  at ambient pressure (30 min, curve b), which increases the number of  $O_2$  molecules passing through the catalyst bed by more than two orders of magnitude compared to the 2000 pulses, led to an about 16 times higher oxygen uptake ( $\sim 1.8 \times 10^{19}$  O atoms  $g_{Au}^{-1}$ ) on the same sample than  $O_2$  pulsing (2000 pulses). A similar experiment, where the reduced NPG catalyst was exposed for 300 min to the 10%  $O_2/N_2$  stream, showed that the oxygen uptake can be further enhanced by prolonging the exposure time ( $\sim 2.5 \times 10^{19}$  O atoms  $g_{Au}^{-1}$ ). The effective probability for active oxygen formation in that experiment is at around  $1.4 \times 10^{-6}$  (total exposure 0.027 mol  $O_2$ ). These results clearly demonstrate that the additional uptake of active oxygen on the NPG catalyst decreases with increasing  $O_2$  exposure but does not saturate in the exposure range tested here.

The different amounts of  $O_2$  activation on the NPG catalyst in the TAP reactor and in flow reactor measurements may result either from the large difference in  $O_2$  exposure between these experiments or from the pressure difference. The total amount of  $O_2$  molecules passing through the catalyst bed is about  $1.6 \times 10^3$  times higher in the flow reactor measurement (30 min) than in the pulse experiments with 200 pulses. We can estimate the total amount of active O atoms deposited during continuous  $CO_2$  formation from the  $CO_2$  formation rate under atmospheric pressure (partial pressures for CO and  $O_2 \sim 10$  kPa each). Under steady-state conditions, the O formation rate is equivalent to the  $CO_2$  formation rate. Using the reaction rate of the micro-reactor measurements, we can estimate that for  $5 \times 10^{15}$   $O_2$  molecules passing through a catalyst bed with 2 mg Au, which is identical to the number of  $O_2$  molecules per pulse and catalyst mass in the TAP reactor measurements, about  $4 \times 10^{14}$  O atoms are deposited and reacted away. In the TAP reactor measurements, a similar amount is deposited in 200 pulses. If in the first pulse, on the reduced NPG sample,

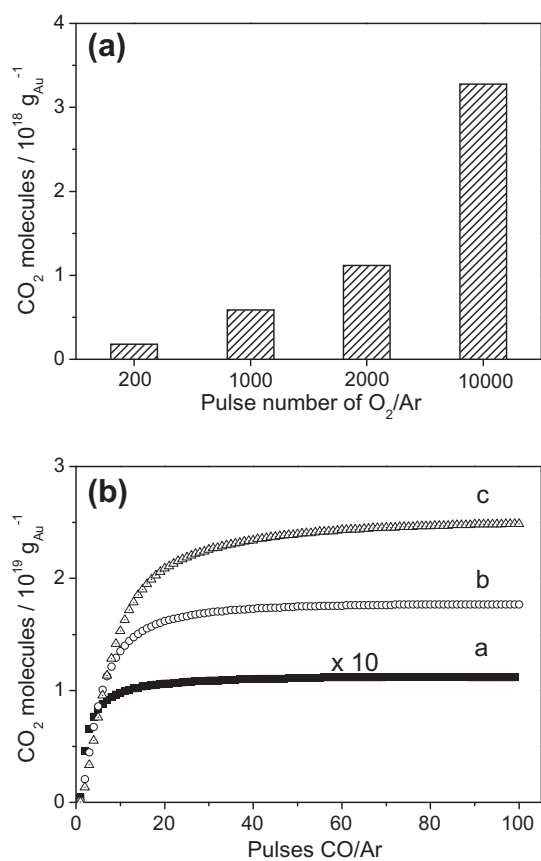


**Fig. 5.** (a) Effect of the number of  $O_2/Ar$  pulses on the amount of  $CO_2$  produced on NPG catalyst. (b) Accumulated amount of  $CO_2$  produced on the NPG catalyst after exposure to 2000 pulses of  $O_2/Ar$  (trace a), after exposure to 10%  $O_2/N_2$  (20 Nml  $min^{-1}$ , atmospheric pressure) for 30 min (trace b), and after exposure to 10%  $O_2/N_2$  (20 Nml  $min^{-1}$ , atmospheric pressure) for 300 min (trace c).

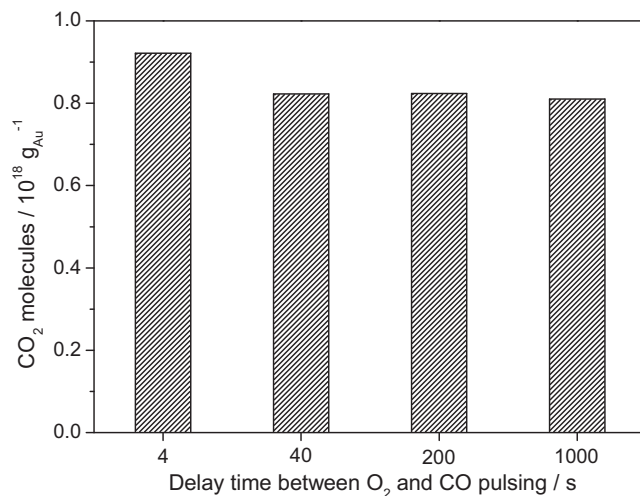


**Fig. 6.** Accumulated amount of  $CO_2$  produced by 50 pulses of  $CO/Ar$  following 1000 pulses of  $O_2/Ar$  with different time delays.

about 10% of that were deposited, this would correspond to  $4 \times 10^{13}$  O atoms. This is less than 0.5% of the  $O_2$  pulse intensity ( $5 \times 10^{15}$   $O_2$  molecules) and below the detection limit, both for  $O_2$  consumption and for  $CO_2$  formation, in agreement with observation during simultaneous pulse measurements. In that case, the number of active oxygen atoms deposited during continuous reaction under atmospheric pressure conditions would be tenfold higher than during pulse deposition for an identical number of  $O_2$  molecules passed through the catalyst bed. Neglecting effects resulting from different contact times, this points to a significant non-linear pressure effect in  $O_2$  activation. A more quantitative statement, however, is not possible at present because of the assumptions underlying the above comparison.

Furthermore, we investigated the stability of the adsorbed activated oxygen species on a new sample by varying the delay time (under UHV conditions) between  $O_2$  pulses (1000 pulses, oxygen accumulation) and subsequent CO pulsing (oxygen reduction) between 4 s and 1000 s (Fig. 6). Similar methods to study the stability of intermediate species have also been applied in TAP studies by other groups [40–45]. Within this time range, there was little variation in the amount of active oxygen species detected on the surface. Hence, at 30 °C and under UHV conditions, desorption of adsorbed active oxygen from the NPG surface is very slow, indicating that this species is stable at 30 °C. This stability points to an atomic O species as active oxygen.

To gain further insight into the mechanism of CO oxidation, we carried out similar TAP measurements using labeled  $^{18}O_2$ . Exposing a fresh (unreduced) NPG catalyst at 30 °C to  $^{18}O_2$  pulses, we did not observe any formation of  $^{16}O^{18}O$ . This rules out the possibility of oxygen exchange between gas-phase  $^{18}O_2$  and pre-existent surface oxygen. In a second isotope labeling experiment, a fresh NPG catalyst was exposed to simultaneous pulses of  $C^{16}O$  and  $^{18}O_2$ . Fig. 7 depicts the pulse responses of reactants and products during this measurement. The almost constant intensity of the  $^{18}O_2$  pulses with time clearly shows that there was only negligible consumption of  $^{18}O_2$ . On the other hand,  $CO_2$  formation was dominated by non-labeled  $C^{16}O_2$ , with only a very small amount of labeled  $C^{16}O^{18}O$  formation. No  $C^{18}O_2$  was detected during the reaction. These results fully support our previous conclusion that active oxygen formation during  $O_2$  pulsing is negligible and that under present reaction conditions (simultaneous CO and  $O_2$  pulsing)  $CO_2$

formation is caused by a non-catalytic reaction, by reaction with the pre-existent surface oxygen.

Subsequently, we investigated the formation of active adsorbed oxygen in a multi-pulse experiment using isotope-labeled  $^{18}O_2$ . Sequences of 200  $C^{16}O$  and 200  $^{18}O_2$  pulses were admitted alternately into the reactor for 64 times without interruption, starting with a pulse-reduced, fresh NPG sample. The accumulated amount of  $CO_2$  formation (Fig. 8a) and the  $C^{16}O^{18}O/C^{16}O_2$  product ratio (Fig. 8b) during the CO pulse sequences are plotted in Fig. 8. During this multi-pulse experiment, only pulse responses from  $C^{16}O_2$  and  $C^{16}O^{18}O$  could be detected in the gas-phase products. As illustrated in Fig. 8, the amount of  $C^{16}O_2$  in the product decreased rapidly from  $0.56 \times 10^{18}$  O atoms  $g_{Au}^{-1}$  to  $0.20 \times 10^{18}$  O atoms  $g_{Au}^{-1}$  within the first 20 cycles and then reached a steady-state value of about  $0.17 \times 10^{18}$  O atoms  $g_{Au}^{-1}$ . The  $C^{16}O^{18}O$  production, in contrast, remained almost constant ( $\sim 0.05 \times 10^{18}$  O atoms  $g_{Au}^{-1}$ ). Note that the  $C^{16}O_2$  production was still decreasing, although the trend is getting smooth. This phenomenon is explained by diffusion-limited segregation of subsurface/bulk oxygen to the surface. This interpretation is supported by the observation (not shown) that for longer reduction sequences in multi-pulse experiments with 2000 pulses of CO, the amount of O removal is comparable to that removed in 200 pulses (slow oxygen segregation rather than CO exposure is rate limiting). The formation of  $C^{16}O^{18}O$  clearly demonstrates that  $O_2$  activation on the partly reduced NPG catalyst is possible also under UHV conditions. The variation of the  $C^{16}O^{18}O/C^{16}O_2$  product ratio (Fig. 8b) reflects the slow accumulation of  $^{18}O$  surface atoms upon exposure to  $^{18}O_2$  pulses. The probability for active oxygen formation during  $O_2$  pulsing, however, is very low, and even during this extended cycling,  $CO_2$  formation is still dominated by reaction with pre-existent  $^{16}O$  on the surface, which had not been completely depleted in the preceding reduction cycles (CO pulsing). Hence, also these measurements resolve a very low  $O_2$  activation activity of the pulse-reduced NPG catalyst. In addition, they demonstrate that after pulse reduction, there are still considerable amounts of oxygen in the surface near region of the sample, which are not accessible for reaction with CO during CO pulsing, but which move to the surface and become accessible to CO upon re-exposure to  $O_2$ , in this case  $^{18}O_2$ . Hence, re-deposition of oxygen, in this case of  $^{18}O$ , activates segregation of subsurface oxygen (in this case  $^{16}O$ ) to the surface, and this process is

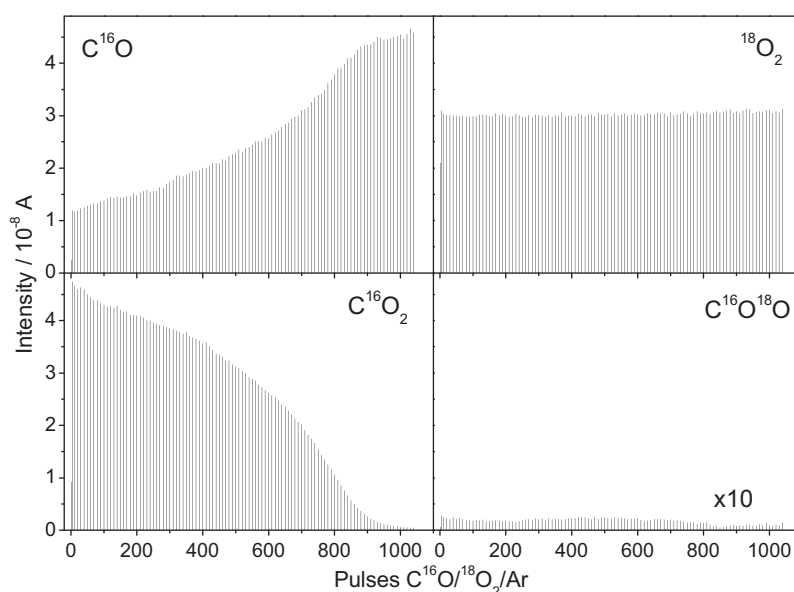
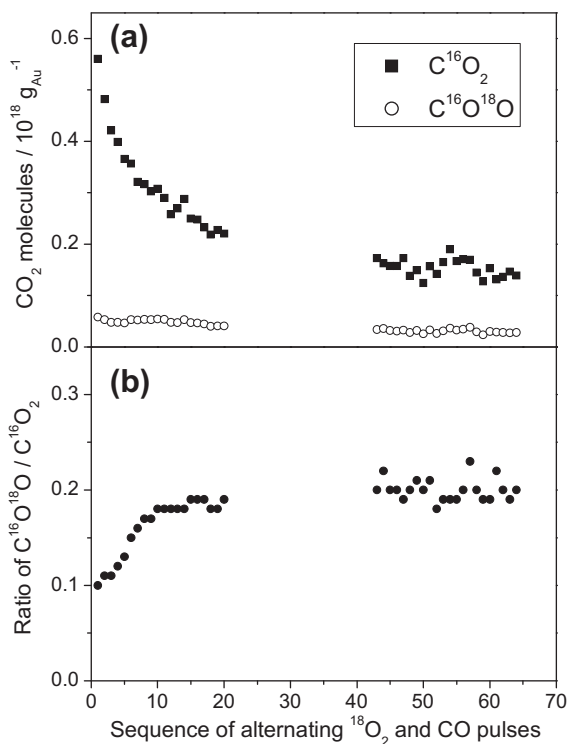


Fig. 7. Sequences of pulse responses during a simultaneous pulse experiment over a NPG catalyst using labeled  $^{18}O_2/Ar$  and  $C^{16}O/Ar$  (reaction temperature 30 °C).



**Fig. 8.** Evolution of  $C^{16}O^{18}O$  and  $C^{16}O_2$  production (a) and the ratio of  $C^{16}O^{18}O / C^{16}O_2$  (b) during multi-pulse cycles upon repeated alternating pulsing of  $^{18}O_2/Ar$  and  $CO/Ar$  sequences over a pre-reduced NPG catalyst.

much more efficient than  $^{18}O$  deposition. Accordingly, subsequent CO pulsing results mainly in  $C^{16}O_2$  formation, although with increasing depletion of subsurface  $^{16}O$  species the surface oxygen-induced segregation process becomes less and less efficient.

The activation of molecular  $O_2$  is a central topic for the reaction mechanism of Au-catalyzed oxidation reactions. For oxide-supported gold catalysts, the perimeter sites at the interface between Au and oxide were frequently referred to as the main active sites for  $O_2$  activation [1–4,8,9,13–16], and this was indirectly verified in recent TAP reactor experiments [13]. The exact nature of the active oxygen species, however, is still unresolved. The existence of such interfacial sites is obviously not possible on NPG catalysts, and therefore, the reaction should be dominated by another mechanism. Despite of the absence of Au-oxide interface sites, the results of the TAP measurements presented in this work provide clear experimental evidence for the formation of stable adsorbed, active oxygen species upon  $O_2/Ar$  pulsing, and based on their stability, these were identified as atomic species. In theory, the atomic O species can be produced under reaction conditions via two possible routes: (1) by dissociative activation of  $O_2$  on the Ag atoms or on Au atoms, possibly facilitated by the presence of atomic oxygen on the surface [10] and (2) by reaction of CO with molecular activated oxygen species, leading to a ‘remaining’  $O_{ad}$  intermediate on the surface [13]. Since the remaining  $O_{ad}$  can easily be removed by another CO molecule, it is not likely that the second route contributed to the formation of stable atomic oxygen species on the NPG surface. Furthermore, the second pathway would not be accessible in multi-pulse experiments and can hence be disregarded as major contribution for active oxygen formation.

From experimental and theoretical studies, it is known that the adsorption and activation of molecular  $O_2$  on Au surfaces is only possible if large fractions of low coordinated gold atoms are present [11,12]. For example, based on the results of DFT calculations, Liu et al. [46] have pointed out that  $O_2$  dissociation on Au atoms

cannot occur at low temperatures but may be possible at elevated temperature. Roldán et al. [47] calculated that low coordinated Au atoms are not sufficiently active to dissociate  $O_2$ . In a recent study, Deng et al. reported that the probability for dissociative adsorption of  $O_2$  at 400 K can be increased by more than 1000 times by pre-deposition of atomic oxygen on a Au(1 1 1) surface [10]. In order to investigate the influence of pre-deposited atomic oxygen on the CO oxidation activity of NPG catalysts, we reduced the NPG catalyst prior to a continuous reaction experiment in a micro-reactor by exposing it to a gas mixture of 1%CO/ $N_2$  (60 ml  $min^{-1}$ ) for 1 min, then changed to a 1%CO/1% $O_2$  in  $N_2$  reaction mixture and monitored the  $CO_2$  formation rate with time (Fig. 9). The results show that the initial activity of the pre-reduced NPG catalyst ( $\sim 1.4 \times 10^{-4} mol_{CO} s^{-1} g_{Au}^{-1}$ ) is somewhat lower than that of an unreduced catalyst (Fig. 2a,  $1.8 \times 10^{-4} mol_{CO} s^{-1} g_{Au}^{-1}$ ). Switching off the  $O_2$  gas supply after 400 min reaction, the reaction rate instantaneously decreased to below measurable values; re-admitting it 30 min later, it returned to an even higher level and then decayed within 50 min to its previous value. The reason for the initially higher  $CO_2$  formation rates is not yet clear, it may partly be caused by an overshoot in the  $O_2$  concentration in the reactant mixture when switching on the  $O_2$  gas supply, but other effects may contribute as well. Overall, however, the reduction of the NPG catalyst during exposure to 1%CO/ $N_2$  for 30 min had no significant influence on the CO oxidation activity and definitely did not cause a major loss of activity. This result is consistent with findings by Xu et al. [20], who also introduced CO/ $N_2$  mixed gas into the micro-reactor to reduce possible gold oxides on NPG prior to the admission of the CO/ $O_2$  reaction gas mixture and found that the activity was not affected by the pre-reduction. Therefore, these results demonstrate that the presence of pre-existent surface oxygen is not a prerequisite for the activation of  $O_2$  on NPG catalyst for reaction/oxygen adsorption under atmospheric pressure conditions. Furthermore, the results from the experiments presented in Figs. 2a, 4 and 9 in combination indicate that there is a loss in OSC during the reaction, in particular during the initial stage, which, however, affects the activity only to a limited extent. Contributions from other effects such as formation of stable surface intermediates, as observed for reaction on oxide-supported Au catalysts [48,49], are likely but cannot be proven from the present data.

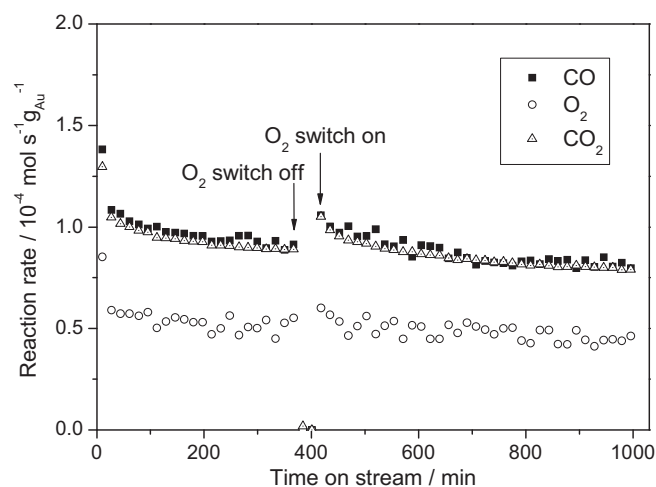


**Fig. 9.** Effect of pre-reduction of the NPG catalyst on the CO oxidation activity measured in the micro-reactor (1 mg catalyst diluted with  $\alpha-Al_2O_3$  (1:60), the catalyst was reduced in 1%CO/ $N_2$  for 1 min before reaction, reaction temperature 30 °C). Furthermore, the  $O_2$  supply was switched off after 400 min on stream and admitted again 30 min later.

The presence of Ag surface and/or subsurface atoms was proposed as a second possibility for promoting the dissociative adsorption of O<sub>2</sub> on Au surfaces [18]. Recently, Chang et al. [50] proposed a reaction pathway via an adsorbed OOCO intermediate for CO oxidation on unsupported, neutral Ag<sub>55</sub>, Au<sub>55</sub> or Ag<sub>30</sub>Au<sub>25</sub> clusters, with an activation barrier of less than 0.5 eV. Based on its higher coadsorption energy for CO and O<sub>2</sub>, the bimetallic Ag<sub>30</sub>Au<sub>25</sub> cluster was anticipated to be a better catalyst for CO oxidation. This effect, however, cannot explain the ability of the NPG catalyst to activate and store active oxygen determined in the multi-pulse experiments. In a combined experimental and theoretical study from the same group, Chou et al. investigated the reaction of CO with AgO added rows on Ag(1 1 0) and Au(1 1 0) surfaces and found an enhanced reactivity for AgO rows on Au(1 1 0) [51]. These observations, however, are little relevant for the actual CO oxidation reaction, where oxygen activation represents the crucial step, while in the above study, oxygen was pre-deposited as atomic species, and both experiment and theory focused on the off-reaction of the pre-deposited oxygen. Nevertheless, an Ag-induced enhancement of O<sub>2</sub> activation appears plausible considering the activity of Ag and Ag catalysts in various oxidation reactions such as epoxidation of ethylene [52–55]. Accordingly, the influence of residual Ag on the activity of NPG catalysts needs to be studied in comparable experiments, which are planned for the future.

#### 4. Conclusions

Based on a combination of static and transient reaction studies, performed in a conventional micro-reactor and in a TAP reactor, we arrived at the following main results and conclusions on the mechanism of the CO oxidation reaction on nanoporous Au:

1. Reaction between a CO/O<sub>2</sub> reaction mixture and an oxygen pre-covered NPG surface (fresh sample) results in a rapid reduction of the catalyst surface and a concomitant decay of the CO oxidation activity of the NPG catalyst in simultaneous pulse experiments, until values below the detection limit (<1% of the initial activity) are reached. Hence, non-catalytic reaction between pre-existent surface oxygen (and surface oxide) and CO, which results in a rapid depletion of surface oxygen, is much faster than re-formation of active oxygen under the reaction conditions in a TAP reactor.
2. Continuous catalytic oxidation of CO is possible during reaction in 1%CO/1% O<sub>2</sub> containing reaction gas at atmospheric pressure. Under these conditions, activation of oxygen is sufficiently fast to result in significant (Au-mass-normalized) reaction rates ( $6.2 \times 10^{-5} \text{ mol}_{\text{CO}} \text{ s}^{-1} \text{ g}_{\text{Au}}^{-1}$  at 30 °C), although they are still lower by a factor of 5 than those of oxide-supported Au/TiO<sub>2</sub> catalysts ( $3.4 \times 10^{-4} \text{ mol}_{\text{CO}} \text{ s}^{-1} \text{ g}_{\text{Au}}^{-1}$  at 30 °C). Comparison of the active oxygen uptake during continuous reaction at atmospheric pressure and during multi-pulse TAP reactor measurements indicates a strongly non-linear dependence of the oxygen activation reaction rate on the oxygen partial pressure.
3. Multi-pulse experiments allowed us to quantify the formation of active adsorbed oxygen during O<sub>2</sub> pulsing or during continuous exposure to O<sub>2</sub>. Depending on the O<sub>2</sub> exposure, active oxygen coverages of up to ~0.022 ML are reached. After 200 pulses of O<sub>2</sub> and repeated oxidation–reduction cycling, the average probability for active oxygen formation was calculated to  $0.2 \times 10^{-3}$ . During continuous exposure to O<sub>2</sub> (maximum total exposure 0.027 mol O<sub>2</sub>), the effective probability for active oxygen formation is  $1.4 \times 10^{-6}$ .
4. Based on its stability (stable at room temperature), the adsorbed active oxygen species is an atomically adsorbed oxygen species. This assignment is corroborated by multi-pulse

experiments using labeled <sup>18</sup>O<sub>2</sub>, which showed a slow increase in the C<sup>16</sup>O<sup>18</sup>O isotopomer during alternating sequences of C<sup>16</sup>O and <sup>18</sup>O<sub>2</sub> pulses. After 64 alternating C<sup>16</sup>O and <sup>18</sup>O<sub>2</sub> sequences, this results in a fraction of 20% <sup>18</sup>O<sub>ad</sub> species of the total amount of surface oxygen accessible for CO oxidation.

5. Effects induced by the presence of Ag in the NPG surface are considered as likely but could not be definitely proven by the present data.

Most important for the comparison with theory is the observation of stable adsorbed active oxygen formation, most likely via dissociative O<sub>2</sub> adsorption, which provides clear evidence that reaction pathways involving CO-induced dissociation of weakly adsorbed O<sub>2,ad</sub> species cannot be the only mechanism for CO oxidation on NPG catalysts. On the other hand, the latter pathway can also not be ruled out as additional pathway from the present data.

#### Acknowledgments

This work was supported by the Baden-Württemberg Stiftung within the Network 'Functional Nanostructures'. L.-C. Wang is grateful for a fellowship from the Alexander-von Humboldt-Foundation. We gratefully acknowledge T. Diemant (Ulm University) for XPS measurements and Y. Zhong (Karlsruher Institute of Technology) for the electrochemical measurements.

#### References

- [1] M. Haruta, T. Kobayashi, H. Sano, N. Yamada, Chem. Lett. 16 (1987) 405.
- [2] M. Haruta, N. Yamada, T. Kobayashi, S. Iijima, J. Catal. 115 (1989) 301.
- [3] M. Haruta, Catal. Surv. Jpn. 1 (1997) 61.
- [4] M. Haruta, Catech 6 (2002) 102.
- [5] G.C. Bond, C. Louis, D.T. Thompson, Catalysis by Gold, Imperial Press, London, 2007.
- [6] G.R. Bamwenda, S. Tsubota, T. Nakamura, M. Haruta, Catal. Lett. 44 (1997) 83.
- [7] M. Valden, X. Lai, D.W. Goodman, Science 281 (1998) 1647.
- [8] M.M. Schubert, S. Hackenberg, A.C. van Veen, M. Muhler, V. Plzak, R.J. Behm, J. Catal. 197 (2001) 113.
- [9] I.N. Remediakis, N. Lopez, J.K. Nørskov, Angew. Chem. 117 (2005) 1858.
- [10] X. Deng, B.K. Min, A. Guloy, C.M. Friend, J. Am. Chem. Soc. 127 (2005) 9267.
- [11] T.V.W. Janssens, A. Carlsson, A. Puig-Molina, B.S. Clausen, J. Catal. 240 (2006) 108.
- [12] N. Lopez, T.V.W. Janssens, B.S. Clausen, Y. Xu, M. Mavrikakis, T. Bligaard, et al., J. Catal. 223 (2004) 232.
- [13] M. Kotobuki, R. Leppelt, D. Hansgen, D. Widmann, R.J. Behm, J. Catal. 264 (2009) 67.
- [14] D. Widmann, R. Leppelt, R.J. Behm, J. Catal. 251 (2007) 437.
- [15] A. Tost, D. Widmann, R.J. Behm, J. Catal. 266 (2009) 299.
- [16] D. Widmann, Y. Liu, F. Schüth, R.J. Behm, J. Catal. 276 (2010) 292.
- [17] V. Zielasek, B. Jürgens, C. Schulz, J. Biener, M.M. Biener, A.V. Hamza, et al., Angew. Chem. Int. Ed. 45 (2006) 8241.
- [18] A. Wittstock, B. Neumann, A. Schaefer, K. Dumbuya, C. Kübel, M.M. Biener, et al., J. Phys. Chem. C 113 (2009) 5593.
- [19] C. Xu, J. Su, X. Xu, P. Liu, H. Zhao, F. Tian, et al., J. Am. Chem. Soc. 129 (2007) 42.
- [20] C. Xu, X. Xu, J. Su, Y. Ding, J. Catal. 252 (2007) 243.
- [21] A. Wittstock, V. Zielasek, J. Biener, C.M. Friend, M. Bäumer, Science 327 (2010) 319.
- [22] S. Parida, D. Kramer, C.A. Volkert, H. Rösner, J. Erlebacher, J. Weissmüller, Phys. Rev. Lett. 97 (2006) 035504-1.
- [23] H.J. Jin, S. Parida, D. Kramer, J. Weissmüller, Surf. Sci. 602 (2008) 3588.
- [24] S. Trasatti, O.A. Petrii, Pure Appl. Chem. 63 (1991) 711.
- [25] M.J. Kahlich, H.A. Gasteiger, R.J. Behm, J. Catal. 171 (1997) 93.
- [26] R. Leppelt, D. Hansgen, D. Widmann, T. Häring, G. Bräth, R.J. Behm, Rev. Sci. Instrum. 78 (2007) 104103.
- [27] J.T. Gleaves, G.S. Yablonskii, P. Phanawadee, Y. Schuurman, Appl. Catal. A 160 (1997) 55.
- [28] H. Rösner, S. Parida, D. Kramer, A. Volkert, J. Weissmüller, Adv. Eng. Mater. 9 (2007) 535.
- [29] G.K. Wertheim, S.B. DiCenzo, S.E. Youngquist, Phys. Rev. Lett. 51 (1983) 2310.
- [30] J.-J. Pireaux, M. Liehr, P.A. Thiry, J.P. Delrue, R. Caudano, Surf. Sci. 141 (1984) 221.
- [31] G.B. Hoflund, Z.F. Hazos, Phys. Rev. B 62 (2000) 11126.
- [32] A.-Q. Wang, J.-H. Liu, S.D. Lin, T.-S. Lin, C.-Y. Mou, J. Catal. 233 (2005) 186.
- [33] R.B. Grant, R.M. Lambert, Surf. Sci. 146 (1984) 256.
- [34] C.T. Campbell, Surf. Sci. 157 (1985) 43.
- [35] C. Rehren, G. Isaac, R. Schlögl, G. Ertl, Catal. Lett. 11 (1991) 253.
- [36] A.G. Sault, R.J. Madix, C.T. Campbell, Surf. Sci. 169 (1986) 347.



- [37] N. Saliba, D.H. Parker, B.E. Koel, *Surf. Sci.* 410 (1998) 270.
- [38] B.K. Min, A.R. Alemozafar, D. Pinnaduwaage, X. Deng, C.M. Friend, *J. Phys. Chem. B* 110 (2006) 19833.
- [39] Y. Denkwitz, Z. Zhao, U. Hörmann, U. Kaiser, V. Plzak, R.J. Behm, *J. Catal.* 251 (2007) 363.
- [40] M. Olea, M. Kunitake, T. Shido, Y. Iwasawa, *Phys. Chem. Chem. Phys.* 3 (2001) 627.
- [41] J. Pérez-Ramírez, E.V. Kondratenko, M.N. Debbagh, *J. Catal.* 233 (2005) 442.
- [42] A. Goguet, S.O. Shekhtman, R. Burch, C. Hardacre, F.C. Meunier, G.S. Yablonsky, *J. Catal.* 237 (2006) 102.
- [43] J. Pérez-Ramírez, E.V. Kondratenko, G. Novell-Leruth, J.M. Ricart, *J. Catal.* 261 (2009) 217.
- [44] A. Kumar, V. Medhekar, M.P. Harold, V. Balakotaiah, *Appl. Catal. B: Environ.* 90 (2009) 642.
- [45] A. Kumar, M.P. Harold, V. Balakotaiah, *J. Catal.* 270 (2010) 214.
- [46] Z.-P. Liu, P. Hu, A. Alavi, *J. Am. Chem. Soc.* 124 (2002) 14770.
- [47] A. Roldan, S. Gonzalez, J.M. Ricart, F. Illas, *Chem. Phys. Chem.* 10 (2009) 348.
- [48] B. Schumacher, Y. Denkwitz, V. Plzak, M. Kinne, R.J. Behm, *J. Catal.* 224 (2004) 449.
- [49] Y. Denkwitz, B. Schumacher, G. Kucerova, R.J. Behm, *J. Catal.* 267 (2009) 78.
- [50] C.M. Chang, C. Cheng, C.-M. Wei, *J. Chem. Phys.* 128 (2008) 124710.
- [51] J.P. Chou, W.W. Pai, C.C. Kuo, J.D. Lee, C.H. Lin, C.-M. Wei, *J. Phys. Chem. C* 113 (2009) 13151.
- [52] J.A. Rodriguez, D.W. Goodman, *Surf. Sci. Rept.* 14 (1991) 1.
- [53] S.R. Bare, *J. Vac. Sci. Technol. A* 10 (1992) 2336.
- [54] H. Nakatsuji, Z.M. Hu, H. Nakai, K. Ikeda, *Surf. Sci.* 387 (1997) 328.
- [55] H. Nakatsuji, H. Nakai, K. Ikeda, Y. Yamamoto, *Surf. Sci.* 384 (1997) 315.